

Green Synthesis of Nickel Nanoparticles Using *Lawsonia inermis* Extract and Evaluation of Their Effectiveness against *Staphylococcus aureus*

Kamal A. Lazim ^{a, } and Hossain M. Moghaddam ^{a, }

^aDepartment of Physics, College of Science, University of Mazandaran, Mazandaran, Iran

CORRESPONDANCE

Kamal A. Lazim
kamalabd.80@gmail.com

ARTICLE INFO

Received: December 08, 2024

Revised: March 15, 2025

Accepted: March 20, 2025

Published: March 30, 2025



© 2025 by the author(s).
Published by Mustansiriyah
University. This article is an
Open Access article distributed
under the terms and condi-
tions of the Creative Com-
mons Attribution (CC BY) li-
cense.

ABSTRACT: *Background:* Nanoparticle synthesis uses the green synthesis of nickel nanoparticles (Ni-NPs) because of its low cost, safety, environmental friendliness, simplicity, and ability to treat environmental pollution. *Objective:* The goal of this work is to make Ni-NPs from *Lawsonia inermis* (henna) extract so that they can kill bacteria by the diffusion method. *Methods:* We synthesized Ni-NPs using the hydrothermal method, determining their structure and optical properties through XRD patterns, FESEM images, and UV-visible spectrum analysis. However, the study of the effect of Ni-NPs synthesized from henna extract on antibacterial activity is ongoing. *Results:* the XRD pattern results proved that the Ni-NPs were synthesized without any other impurities. The FESEM results revealed that the Ni-NPs exhibited a nano-spherical-like shape, with nano-diameters ranging from 11.16 to 401 nm. The optical properties of Ni-NPs are determined by the UV-visible spectrum. The absorbance value of the Ni-NPs synthesized using the henna leaves extract exhibited from 250-290 nm in the UV-Vis spectrum. The inhibition of zone values between 29 and 34 mm on antibacterial activity using Ni-NPs. *Conclusions:* The results for the diffusion technique showed that because of its improved structure and optical properties, Ni-NPs are a very effective activity material for bacteria.

KEYWORDS: Green synthesis; Nickle nanoparticles; Hyderothermal; Antibacteria; Henna

INTRODUCTION

The green synthesis of Ni-NPs has the potential to open up new avenues by using *Lawsonia inermis* (henna) leaf extract mining as a capping and reducing agent to produce cheaper, cleaner, and more environmentally friendly NPs. Furthermore, as biological materials are abundantly available, green synthesis now contributes to their substantial pharmaceutical usage in the industry with increased attention. Nanotechnology is expected to play a significant role in the biomedical industry by preventing and treating illnesses using atomic-scale materials [1], [2]. Ni-NPs are chemically stable and possess excellent electro-optical properties, including a large band gap (3.6-4.6 eV) [3]. Ni-NPs have also been shown to have antimicrobial properties. Ni is a P-type semiconductor that has a wide variety of applications in both the chemical and physical realms. Some of these applications include catalysis, solar cells, and gas sensors [4]–[6]. Ni-NPs can be prepared using a number of different routes, some of which have been documented in the literature (such as thermal decomposition). Some of the techniques that can be employed include combustion [7], sol-gel [8], co-precipitation [9], spray pyrolysis [10], and the anodic arc plasma technique [11]. Green synthesis is cost-effective and ecologically friendly since it does not require a lot of energy, high temperatures, or harmful chemicals. It can also be readily scaled up for large-scale synthesis, providing it an advantage over other approaches. Green synthesis allows for more precise control over crystal formation. Low-cost and flexible, NPs manufactured utilizing environmentally friendly technologies have several potential applications in the scientific community [12].

In recent years, hydrothermal processing has emerged as an alternative processing technology for moist biomass and waste Materials. Materials with an elevated energy density can be produced by employing hot-compressed water as a reaction medium at temperatures ranging from 200°C to 500°C. The technology is particularly well-suited for damp and waste materials, as it does not necessitate the dehydration of the feedstock [13]. The objective of this investigation was to develop a novel eco-synthesis of Ni-NPs that employs a byproduct of henna leaf extract as the green agent. The stability of nanoparticles is guaranteed by the presence of significant quantities of plant extract phytoconstituents, including terpenoids, flavonoids, steroids, sapogenins, amino acids, carbohydrates, and polypeptides, which function as both reducing and capping agents [14]. Gallic acid and Lawsonia (2-hydroxy 1,4-naphthoquinone) are two critical components of henna extract that are believed to function as reducing agents [15].

The literature survey shows the difference in this work compared to others. A 2024 study (Fasial J. *et al.* [16]) included shrimp extracts for the synthesis of silver oxide nanoparticles using two methods (hydrothermal method and PLA technique) for antibacterial activity. A 2025 iron oxide/graphene oxide nanoparticles were prepared from the *myrtus* extract using two methods (hydrothermal method and PLA technique) for gas sensor activity [17].

This work involved the hydrothermal synthesis of Ni-NPs from henna extract and nickel (II) nitrate $\text{Ni}(\text{NO}_3)_2$. The synthesized Ni-NPs were characterized using X-ray diffraction. This was one of the ways used to validate the physical and chemical characteristics of the manufactured Ni-NPs using XRD (XRD6000 Shimadzu Company / Japan). A (SHAMIZDA-1800UV) spectrometer is utilized to evaluate the UV-visible spectrum. The particle size and morphology of Ni NPs are determined using FE-SEM via (JAEL JSM-6460LV). The novelty of this work preparation of nickel nanoparticles from the henna extract by hydrothermal method for antibacterial activity.

MATERIALS AND METHODS

On a local market of the henna extract (Baghdad, Iraq), and Ni_2NO_3 salt (China, 99.9%). The henna excels in its capabilities of nitrogen and phosphorous is as high as the amount of henna extract and is a reduction, stabilization, and clumping agent that enables the production of huge amounts of nanoparticles. All solutions are made using distilled water.

Synthesis of henna Extract

The henna leaves were thoroughly washed with distilled water to remove impurities and then sun-dried for two days. After drying, the leaves were finely ground using an electric grinder to obtain a uniform powder. To prepare the extract, (5 grams) of the henna powder was mixed with 100 ml of distilled water and heated at 60 °C for 1 hour. The concentration of the plant is 50000 ppm. The resulting mixture was then cooled to room temperature and filtered using standard filter paper to obtain a clear extract for further use [18], [19].

Synthesis of Ni-NPs using henna Extract

Nickel nanoparticles (Ni-NPs) were synthesized using henna leaf extract. A solution of 100 ml of distilled water to (1M, 6.5 g) of hydrate nickel salt $\text{Ni}(\text{NO}_3)_2$ was prepared and mixed with 100 ml of the henna extract. The mixture was heated to 80 °C on a hot plate stirrer for 50 minutes. During the synthesis process, a notable color change was observed, transitioning from translucent off-green to brown, indicating the formation of Ni-NPs. The resultant solution was allowed to cool at room temperature and then refrigerated. To obtain the Ni-NP nano-powder, 20 ml of the Ni-NPs solution was transferred to an autoclave and subjected to hydrothermal treatment at 180 °C for 18 hours. The purpose of processing the material at 180 °C to control the size and shape of the nanomaterials. Finally, the Ni-NP solutions were stored in sealed serum tubes for further characterization [20].

Antibacterial Activity

Bacterial culture containers exhibited a dose-dependent suppression of zone formation, which was elucidated by Ni-NPs. An intrinsic property of Ni-NPs synthesized from henna extract using a hydrothermal method (*S. aureus*) is their high zone inhibition against gram-positive bacteria. Gram-positive bacteria possess a dense peptidoglycan layer that contains lipopolysaccharides, phospholipids, and proteins, which may account for the observed variation in cell wall structure. This enables a comprehensive understanding of the bactericidal activity of the Ni-NPs that are produced, which is

entirely contingent upon the thickness of the cell dike, the morphology of the cell enveloping, and the resistance of the external membrane to the ROS produced by metal ions. The antimicrobial effect of NPs was demonstrated through a variety of methods, such as the emission of sublime metals and DNA, the descent of interacting oxygen species, and cell membrane injury, all of which inhibit the aerobic series and cell sections. Cell spilt, exocytosis, or DNA insertion/inactivation of key enzymes are all detrimental to the developing cell and can be induced by internalization. The inhibitory zone proportion was determined by employing the subsequent equation [21]:

$$\text{Inhibition Zone (\%)} = \frac{\text{Diameter of the inhibition zone in mm}}{\text{Diameter of petriplate (90 mm)}} \times 100\% \quad (1)$$

RESULTS AND DISCUSSION

Analyzing Crystallin Structure XRD, SEM Analysis, and UV-visible

The compositions and crystallinity of the as-prepared materials are distinguished using the XRD pattern, which is a widely used method. With space group (Fm-3m), crystal dimensions ($a = b = c = 4.193 \text{ \AA}$), crystal angles ($\alpha = \beta = \gamma = 90^\circ$), and the main peaks corresponding to planes (111), (200), and (220), Figure 1 and Table 1 show how the cubic Ni-NPs crystal structure and the crystal size were formed. The sharp diffraction peak that was visible in the pattern could be precisely indexed to the cubic structure of Ni with the cell constant, which corresponded to JCPDS card No. 7440-02-0. The cubic phase of Ni-NP underwent a development of approximately 180°C , as indicated by the XRD data, and the peaks became more pronounced. This is a common characteristic of all materials that are produced using the hydrothermal method. The cubic crystal form of Ni-NPs was observed in the XRD readings at 180°C . The crystallite size has been determined using Scherer's equation, this result agrees with the reference [22].

$$D = \frac{k \lambda}{\beta \cos \theta} \quad (2)$$

where D represents the size of the crystallite, λ is the wavelength of the X-ray (1.5406 \AA), β is the full width at half maximum (FWHM) of the peaks, k is Scherer's constant and is equivalent to 0.9 for spherical particles, and θ is the diffraction angle.

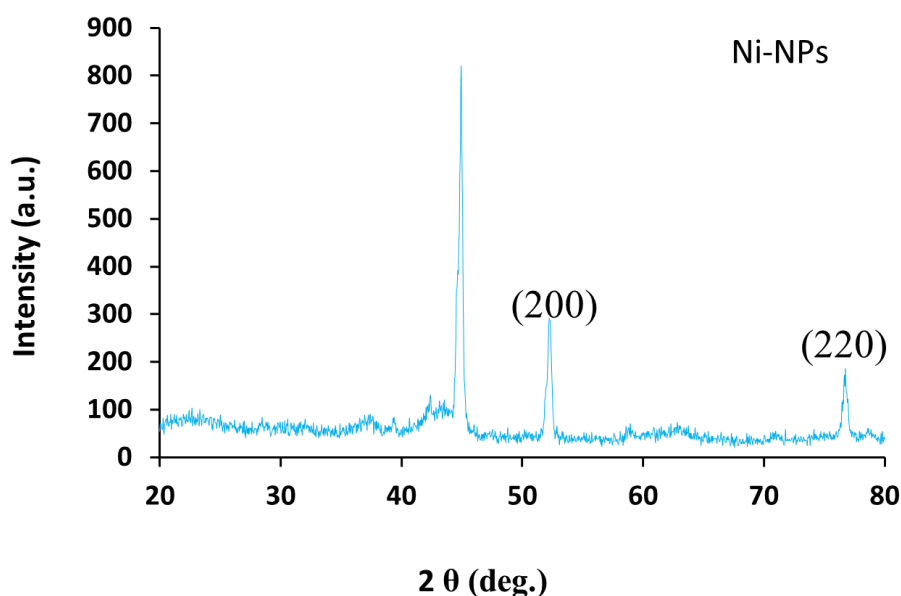
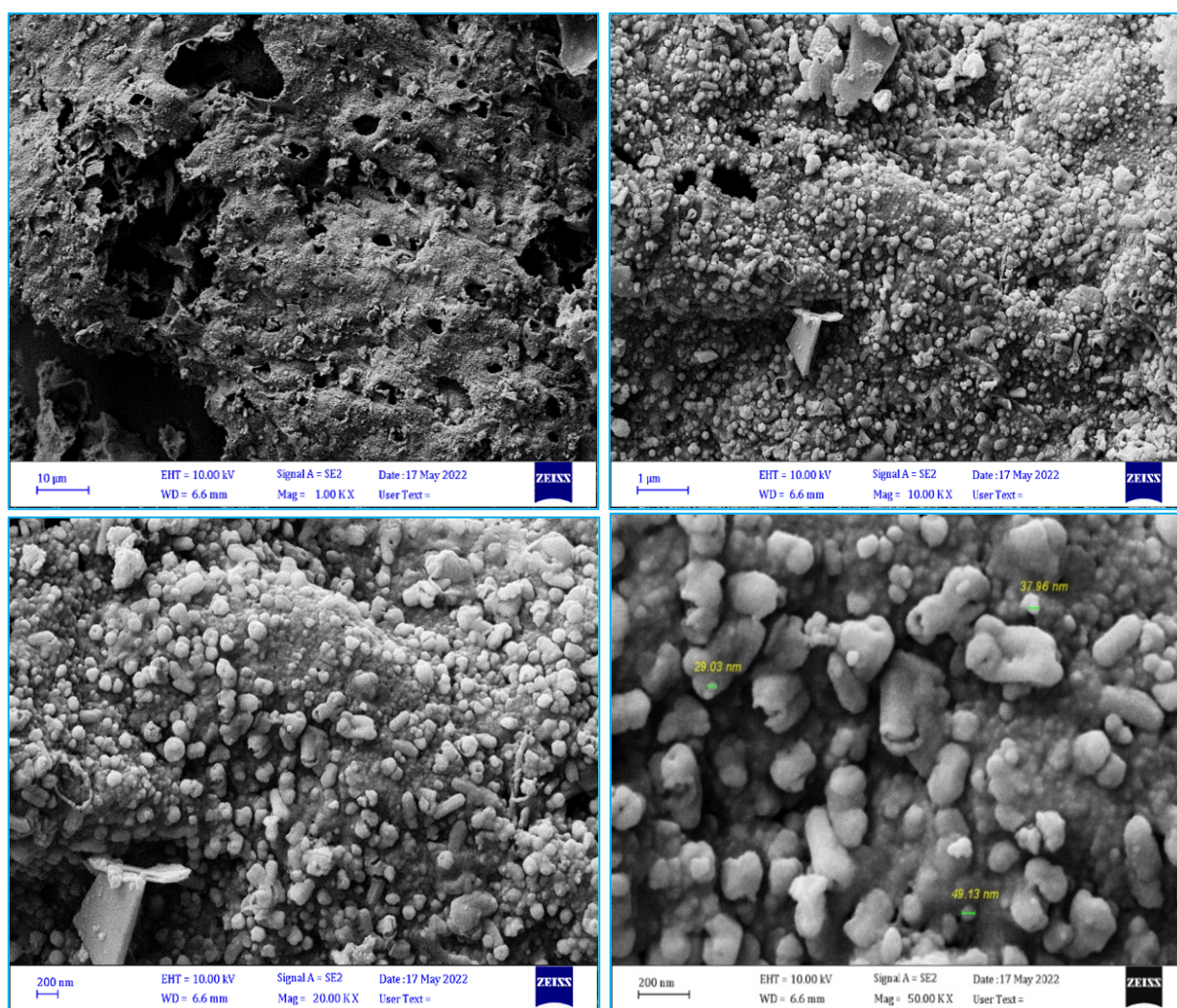


Figure 1. XRD of Ni-NPs

Table 1. XRD patterns of Ni-NPs synthesized by a hydrothermal process at 180 °C

Material	Plant Extract	(hkl)	2 θ (deg.)	FWHM β (deg.)	Crystallite Size D (nm)
Ni	<i>henna</i>	(111)	44.5	0.45	18.98406
		(200)	51.8	0.32	27.47611
		(220)	76.8	0.87	11.61914

Field emission scanning electron microscopy (FE-SEM) is a sophisticated technology that is employed to obtain the microstructure image of the materials. The morphological structure of the reaction products is evaluated using FE-SEM microscopy during the green synthesis of metal nanoparticles. Figure 2 illustrates the morphological transformation that occurs over a period of 18 hours at a temperature of 180 °C. Temperature appears to have a substantial impact on the size and distribution of the particles, as well as the geometry of the structure. The morphology, which also influences the shape of Ni-NPs, explains the homogeneous distribution of the particles. The product of Ni-NPs at 180 °C is comparatively uniform, as illustrated in Figure 2, this result agrees with [23]. These NPs combined to produce nanoparticles and a nano-spherical-like morphology with diameters ranging from 29 to 49 nm.

**Figure 2.** FE-SEM images of Ni-NPs

UV-Vis spectroscopy is an analytical technique that is cost-effective, uncomplicated, versatile, non-

destructive, and suitable for a wide range of organic compounds and certain inorganic species. The optical absorbance spectra of Ni-NPs formed on a glass substrate using an autoclave hydrothermal technique with (henna) extract at 180 °C are displayed in Figure 3. The high absorbance percentage of 347 nm in Figure 3, according to [24] is indicative of the substantial absorbance of (Ni) in this region and the spectral range (200-900 nm). The observed variance in the optical band gap may be attributed to the average crystallite size change of the material, as observed in XRD [25].

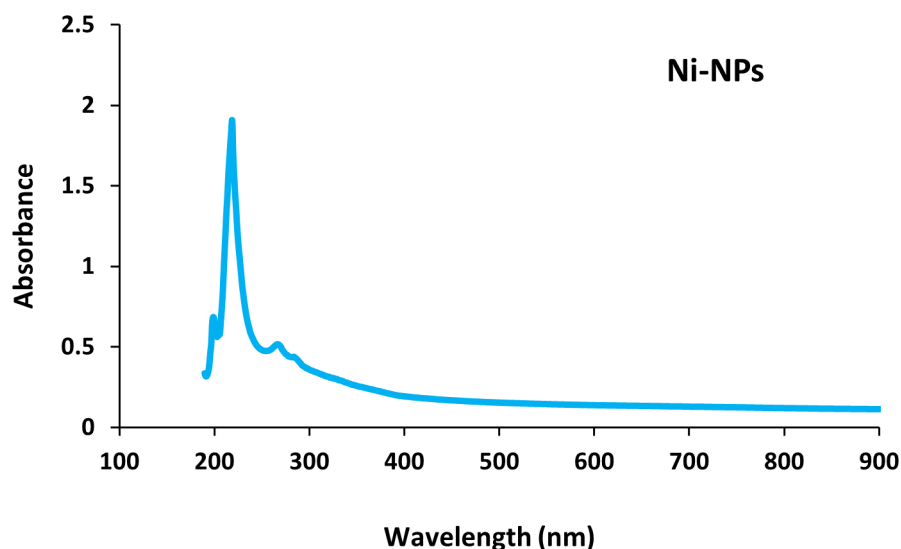


Figure 3. UV-Vis absorbance spectrum of Ni-NPs

Antibacterial Activity

Researchers have looked at how well Ni-NPs that were made by heating henna extract at 180 °C in water can kill bacteria. The standard bacteria that have been tested for antibacterial activity are *S. aureus* (burn and sputum) and other Gram-positive bacteria. The effectiveness of the antibacterial action has been measured by the number of inhibition zones (mm). At 180 °C, the biosynthesis of Ni-NPs worked better than that of metal salt and henna extract. The biosynthesis of NPs also showed a good level of inhibition [26]. When the henna extract is heated to 180 °C, it releases Ni ions that are drawn to the cell wall of bacteria by electrostatic forces. This is what makes the Ni-NPs antibacterial. Moreover, the metal ions have the ability to enter the bacteria and interact with their surface as well. The thiol group (-SH) in the bacterial cell wall may react with NPs, preventing nutrients from passing through it. Cellular death results from a reduction in protein within the cell [27].

In contrast, smaller metal nanoparticles (NPs) are associated with a greater band gap. This suggests that the production of a higher concentration of reactive oxygen species (ROS) will boost antibacterial activity by enhancing exciton accessibility. However, the activity depended on a lot of surface area compared to volume, the concentration of NPs, their crystalline structure, and the shape of the particles [28]–[30]. Table 2 and Figure 4 illustrate that the rate of destruction is lower in relation to metal salt and henna leaves. On the other hand, most bacteria of both types are killed when Ni-NPs are made with henna extract at 180°C. In this case, (1) is Ni₂NO₃ salt, (2) is henna extract, and (3) is Ni-NPs.

Table 2. Result of antibacterial activity

Material	Plant Extract	Temperature(°C)	Gram-positive (+)						Percentage of Inhibition zone (%)						Control
			<i>S. aureus</i>						<i>S. aureus</i>						
			Sputum			Burn			Sputum			Burn			
			1	2	3	1	2	3	1	2	3	1	2	3	
Ni	Henna	180	14	14	34	12	13	24	19	19	39	15	16	29	0

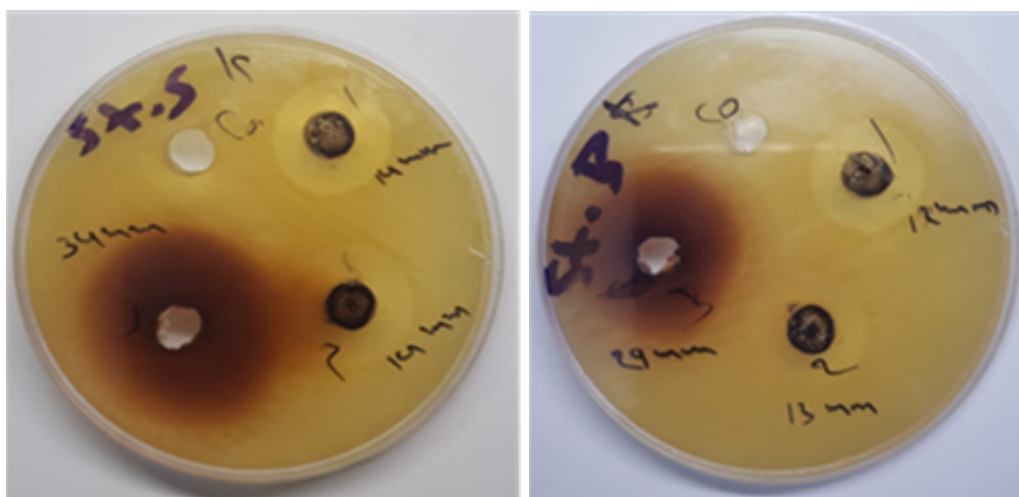


Figure 4. Antibacterial activity of Ni-NPs

CONCLUSION

In this study, Ni-NPs was prepared by combining nickel nitrate $\text{Ni}(\text{NO}_3)_2 \cdot 6\text{H}_2\text{O}$ salt with an extract of henna using the hydrothermal method. The synthesis of Ni-NPs was demonstrated by the changing color of the solutions caused by the henna extract. The utilization of an extract derived from henna leaves as a reducing, stabilizing, and anti-caking agent has been demonstrated to enhance the preparation of Ni-NPs. The optical properties and structure of Ni-NPs were investigated by XRD, FESEM, and UV-visible spectrums. The XRD analysis results indicated that the Ni-NPs generated using the henna leaves extract had a cubic structure and a crystallite dimension ranging from 11 to 17 nm. The FE-SEM images demonstrated that the Ni-NPs was morphology and a nano-spherical-like structure, with a particle size ranging from 29 to 49 nm. The absorbance value of the Ni-NPs synthesized using the henna leaves extract exhibited from 250-290 nm in the UV-Vis spectrum. The antibacterial activity of Ni-NPs was verified through the investigation of the inhibition of zones from 28 to 34 mm using henna leaves extract.

SUPPLEMENTARY MATERIAL

None.

AUTHOR CONTRIBUTIONS

Kamal A. Lazim: Suggested the research idea and methodology; Hossain M. Moghaddam: Investigation, writing, review, and editing.

FUNDING

None.

DATA AVAILABILITY STATEMENT

None.

ACKNOWLEDGMENTS

The authors are grateful to the University of Mazandaran for providing the facilities and constant encouragement for this work.

CONFLICTS OF INTEREST

The authors declare no conflicts of interest.

REFERENCES

- [1] A. Balati, A. Bazilio, A. Shahriar, K. Nash, and H. J. Shipley, "Simultaneous formation of ultra-thin MoSe₂ nanosheets, inorganic fullerene-Like MoSe₂ and MoO₃ quantum dots using fast and ecofriendly pulsed laser ablation in liquid followed by microwave treatment," *Materials Science in Semiconductor Processing*, vol. 99, pp. 68–77, Aug. 2019. doi: 10.1016/j.mssp.2019.04.017.
- [2] M. Vahedi, N. Hosseini-Jazani, S. Yousefi, and M. Ghahremani, "Evaluation of anti-bacterial effects of nickel nanoparticles on biofilm production by *Staphylococcus epidermidis*," *Iranian Journal of Microbiology*, vol. 9, no. 3, pp. 160–168, 2017. [Online]. Available: <https://ijm.tums.ac.ir/index.php/ijm/article/view/915>.
- [3] M. R. Ahghari, V. Soltaninejad, and A. Maleki, "Synthesis of nickel nanoparticles by a green and convenient method as a magnetic mirror with antibacterial activities," *Scientific Reports*, vol. 10, no. 1, p. 12627, 2020. doi: 10.1038/s41598-020-69679-4.
- [4] P. Patra, R. Kumar, C. Kumar, and P. K. Mahato, "Ni-incorporated cadmium sulphide quantum dots for solar cell: An evolution to microstructural and linear-nonlinear optical properties," *Journal of Crystal Growth*, vol. 583, p. 126542, Apr. 2022. doi: 10.1016/j.jcrysgro.2022.126542.
- [5] S. Lokhande, M. Awale, G. Umadevi, and V. Mote, "Effect of Ni doping on structural, optical and gas sensing properties of ZnO films for the development of acetone sensor devices," *Materials Chemistry and Physics*, vol. 301, p. 127667, Jun. 2023. doi: 10.1016/j.matchemphys.2023.127667.
- [6] C. Dhakal, "Synthesis and applications of nickel-based nanomaterials," in *Green Synthesis and Emerging Applications of Frontier Nanomaterials*. Materials Research Forum LLC, Nov. 2024, pp. 139–172. doi: 10.21741/9781644903261-6.
- [7] F. Thema, E. Manikandan, A. Gurib-Fakim, and M. Maaza, "Single phase Bunsenite NiO nanoparticles green synthesis by *Agathosma betulina* natural extract," *Journal of Alloys and Compounds*, vol. 657, pp. 655–661, Feb. 2016. doi: 10.1016/j.jallcom.2015.09.227.
- [8] C. Vidya, S. Hiremath, M. Chandraprabha, M. Antonyraj, I. V. Gopal, A. Jain, and K. Bansal, "Green synthesis of ZnO nanoparticles by *Calotropis gigantea*," *International Journal of Current Engineering and Technology*, vol. 1, no. 1, pp. 118–120, 2013. [Online]. Available: <https://inpressco.com/wp-content/uploads/2013/09/Paper23118-120.pdf>.
- [9] A. Haider, M. Ijaz, S. Ali, J. Haider, M. Imran, H. Majeed, I. Shahzadi, M. M. Ali, J. A. Khan, and M. Ikram, "Green synthesized phytochemically (*Zingiber officinale* and *Allium sativum*) reduced Nickel Oxide nanoparticles confirmed bactericidal and catalytic potential," *Nanoscale Research Letters*, vol. 15, no. 1, p. 50, 2020. doi: 10.1186/s11671-020-3283-5.
- [10] B. H. Shnawa, P. J. Jalil, S. M. Hamad, and M. H. Ahmed, "Antioxidant, protoscolicidal, hemocompatibility, and antibacterial activity of Nickel Oxide nanoparticles synthesized by *Ziziphus spina-christi*," *BioNanoScience*, vol. 12, no. 4, pp. 1264–1278, 2022. doi: 10.1007/s12668-022-01028-3.
- [11] K. Nian, W. Xie, and H. Tu, "Numerical simulation of molten pool flow behavior in ultrasonic vibration-assisted gas tungsten arc welding of low-alloy high-strength steel," *CIRP Journal of Manufacturing Science and Technology*, vol. 55, pp. 347–358, Dec. 2024. doi: 10.1016/j.cirpj.2024.10.012.
- [12] M. Sharma, P. S. Nayak, S. Asthana, D. Mahapatra, M. Arakha, and S. Jha, "Biofabrication of silver nanoparticles using bacteria from mangrove swamp," *IET Nanobiotechnology*, vol. 12, no. 5, pp. 626–632, 2018. doi: 10.1049/iet-nbt.2017.0205.
- [13] P. Biller and A. Ross, "Production of biofuels via hydrothermal conversion," in *Handbook of Biofuels Production*. Elsevier, 2016, pp. 509–547. doi: 10.1016/b978-0-08-100455-5.00017-5.
- [14] P. S. Nayak, S. Pradhan, M. Arakha, D. Kumar, M. Saleem, B. Mallick, and S. Jha, "Silver nanoparticles fabricated using medicinal plant extracts show enhanced antimicrobial and selective cytotoxic propensities," *IET Nanobiotechnology*, vol. 13, no. 2, pp. 193–201, 2018. doi: 10.1049/iet-nbt.2018.5025.
- [15] A. Ebrahiminezhad, S. Taghizadeh, Y. Ghasemi, and A. Berenjian, "Green synthesized nanoclusters of ultra-small zero valent iron nanoparticles as a novel dye removing material," *Science of The Total Environment*, vol. 621, pp. 1527–1532, Apr. 2018. doi: 10.1016/j.scitotenv.2017.10.076.
- [16] F. J. Kadhim, M. H. Bedoui, D. A. Kadhim, and M. A. Abid, "Novel comparison of silver oxide nanoparticle preparation from mixing the wild shrimp extract with Ag₂NO₃ salt via hydrothermal with and without laser for staphylococcus bacteria activity," *Optics & Laser Technology*, vol. 182, p. 112109, Apr. 2025. doi: 10.1016/j.optlastec.2024.112109.
- [17] A. H. A. Raheem, N. Qasim, D. A. Kadhim, and M. A. Abid, "Development of graphene oxide/iron oxide nanocomposite preparation from *Myrtus communis* extract by two methods for the gas sensor application," *Diamond and Related Materials*, vol. 153, p. 112101, Mar. 2025. doi: 10.1016/j.diamond.2025.112101.

- [18] S. Machado, J. Grosso, H. Nouws, J. Albergaria, and C. Delerue-Matos, "Utilization of food industry wastes for the production of zero-valent iron nanoparticles," *Science of The Total Environment*, vol. 496, pp. 233–240, Oct. 2014. doi: 10.1016/j.scitotenv.2014.07.058.
- [19] L. Ren, Y.-P. Zeng, and D. Jiang, "The improved photocatalytic properties of P-type NiO loaded porous TiO₂ sheets prepared via freeze tape-casting," *Solid State Sciences*, vol. 12, no. 1, pp. 138–143, 2010. doi: 10.1016/j.solidstatesciences.2009.09.021.
- [20] A. M. Hamdan, A. Sardi, R. P. Reksamunandar, Z. Maulida, D. A. Arsa, S. S. Lubis, and K. Nisah, "Green synthesis of NiO nanoparticles using a Cd hyperaccumulator (*Lactuca sativa* L.) and its application as a Pb(II) and Cu(II) adsorbent," *Environmental Nanotechnology, Monitoring & Management*, vol. 21, p. 100910, May 2024. doi: 10.1016/j.enmm.2023.100910.
- [21] P. Kathiravan, K. Thillaiavelavan, and G. Viruthagiri, "Influence of Cu-ion doping in NiO NPs and their structural, morphological, optical and magnetic behaviors for optoelectronic devices and magnetic applications," *Spectrochimica Acta Part A: Molecular and Biomolecular Spectroscopy*, vol. 308, p. 123745, Mar. 2024. doi: 10.1016/j.saa.2023.123745.
- [22] A. K. Gatin, S. A. Ozerin, P. K. Ignat'eva, V. A. Kharitonov, S. Y. Sarvadii, and M. V. Grishin, "Adsorption properties of individual Gold, Nickel, and Platinum nanoparticles deposited onto Silicon surface," *Colloid Journal*, vol. 86, no. 4, pp. 519–527, 2024. doi: 10.1134/s1061933x24600507.
- [23] T. Adinaveen, T. Karnan, and S. A. Samuel Selvakumar, "Photocatalytic and optical properties of NiO added *Nephelium lappaceum* L. peel extract: An attempt to convert waste to a valuable product," *Heliyon*, vol. 5, no. 5, e01751, 2019. doi: 10.1016/j.heliyon.2019.e01751.
- [24] P. Kuppusamy, M. M. Yusoff, G. P. Maniam, and N. Govindan, "Biosynthesis of metallic nanoparticles using plant derivatives and their new avenues in pharmacological applications – An updated report," *Saudi Pharmaceutical Journal*, vol. 24, no. 4, pp. 473–484, 2016. doi: 10.1016/j.jsps.2014.11.013.
- [25] M. A. Abid, D. A. Kadhim, and W. J. Aziz, "Iron oxide nanoparticle synthesis using trigonella and tomato extracts and their antibacterial activity," *Materials Technology*, vol. 37, no. 8, pp. 547–554, 2020. doi: 10.1080/10667857.2020.1863572.
- [26] M. A. Abid and D. A. Kadhim, "Novel comparison of iron oxide nanoparticle preparation by mixing iron chloride with henna leaf extract with and without applied pulsed laser ablation for methylene blue degradation," *Journal of Environmental Chemical Engineering*, vol. 8, no. 5, p. 104138, 2020. doi: 10.1016/j.jece.2020.104138.
- [27] M. A. Abid and D. A. Kadhim, "Synthesis of iron oxide nanoparticles by mixing chilli with rust iron extract to examine antibacterial activity," *Materials Technology*, vol. 37, no. 10, pp. 1494–1503, 2021. doi: 10.1080/10667857.2021.1959189.
- [28] A. Zemieche, L. Chetibi, D. Hamana, S. Achour, and V. D. Noto, "Symmetric and asymmetric supercapacitor fabrication based on green synthesized NiO nanoparticles and Graphene," *Colloid Journal*, vol. 86, no. 2, pp. 330–345, 2024. doi: 10.1134/s1061933x23600914.
- [29] A. Umer, S. Naveed, N. Ramzan, M. S. Rafique, and M. Imran, "A green method for the synthesis of Copper nanoparticles using L-ascorbic acid," *Matéria (Rio de Janeiro)*, vol. 19, no. 3, pp. 197–203, 2014. doi: 10.1590/s1517-70762014000300002.
- [30] G. A. Alharshan, A. Almohammed, M. A. M. Uosif, E. R. Shaaban, and M. Emam-Ismail, "Impact of heat treatment on the structural, optical, magnetic and photocatalytic properties of Nickel Oxide nanoparticles," *Materials*, vol. 17, no. 16, p. 4146, 2024. doi: 10.3390/ma17164146.